Mathematical and Computer Modelling 55 (2012) 1876–1891

Contents lists available at SciVerse ScienceDirect

Mathematical and Computer Modelling

journal homepage: www.elsevier.com/locate/mcm

Series solutions of non-Newtonian nanofluids with Reynolds' model and Vogel's model by means of the homotopy analysis method

R. Ellahi [a,b,*], M. Raza [b], K. Vafai [a]

[a] Department of Mechanical Engineering, Bourns Hall, University of California, Riverside, 92521, USA

[b] Department of Mathematics & Statistics, FBAS, IIU, Islamabad, Pakistan

ARTICLE INFO

Article history:
Received 27 September 2011
Received in revised form 14 November 2011
Accepted 15 November 2011

Keywords:
Non-Newtonian nanofluid
Reynolds' model
Vogel's model
Variable viscosity
Porosity effects
Heat transfer analysis
Nonlinear coupled equations
Analytical solutions
Convergence

ABSTRACT

Heat transfer plays an important role in the handling and processing of non-Newtonian nanofluids. In this paper, the fully developed flow of an incompressible, thermodynamically compatible non-Newtonian third-grade nanofluid in coaxial cylinders is studied. Two illustrative models of variable viscosity, namely (i) Reynolds' model and (ii) Vogel's model, are considered. Analytic solutions of velocity, temperature, and nanoparticle concentration are first developed by the homotopy analysis method (HAM), and then the role of pertinent parameters is illustrated graphically. Convergence of the obtained series solutions has been discussed explicitly and the recurrence formulae for finding the coefficients are also given in each case.

1. Introduction

In the last two decades, the study of non-Newtonian fluids [1–7] has gained great importance, and this is mainly due to their huge range of applications. Recent advances in nanotechnology have led to the development of a new innovative class of heat transfer called nanofluids created by dispersing nanoparticles (10–50 nm) in traditional heat transfer fluids [8]. Non-Newtonian nanofluids are widely encountered in many industrial and technology applications, such as melts of polymers, biological solutions, paints, tars, asphalts, and glues, but a careful review of the literature reveals that non-Newtonian nanofluids have so far received very little attention. Nanofluids appear to have the potential to significantly increase heat transfer rates in a variety of areas such as industrial cooling applications, nuclear reactors, transportation industry (an automobiles, trucks, and airplanes), micro-electromechanical systems, electronics and instrumentation, and biomedical applications (nano-drug delivery, cancer therapeutics, cryopreservation). Nanofluids have been found to possess enhanced thermophysical properties such as thermal conductivity, thermal diffusivity, viscosity, and convective heat transfer coefficients compared to those of base fluids like oil or water. The materials which are commonly used as nanoparticles include chemically stable metals (e.g., gold, copper), metal oxides (e.g., alumina, silica, zirconia, titania), oxide ceramics (e.g., Al_2O_3, CuO), metal carbides (e.g., SiC), metal nitrides (e.g., AlN, SiN), carbon in various forms (e.g., diamond, graphite, carbon nanotubes) and functionalized nanoparticles. Some relevant studies on the topic can be found in [9–11].

The study of the behavior of the motion of non-Newtonian nanofluids is complicated and difficult because of the nonlinear relationship between the stress and the rate of strain, and this is due to the fact that most phenomena in the real world are

* Corresponding author at: Department of Mechanical Engineering, Bourns Hall, University of California, Riverside, 92521, USA. Tel.: +1 951 2756747.
E-mail address: ellahi@ucr.edu (R. Ellahi).

0895-7177/$ – see front matter © 2011 Elsevier Ltd. All rights reserved.
doi:10.1016/j.mcm.2011.11.043

essentially nonlinear and are usually described by nonlinear equations. It is very easy to solve a linear problem but finding solutions of nonlinear problems is still very difficult. In particular, getting an exact analytic solution of a given nonlinear problem is often more difficult compared to getting a numerical solution, despite the availability of high-performance supercomputers. However, results obtained by numerical methods give discontinuous points of a curve when plotted; besides that, obtaining the complete necessary understanding of a nonlinear problem is also difficult. If a nonlinear problem contains a singularity or has multiple solutions then this also adds to the numerical difficulties. Though numerical and analytic methods for solving nonlinear problems have limitations, at the same time they have their own advantages too. Therefore, we cannot neglect either of the two approaches but usually it is pleasing to solve a nonlinear problem analytically. Moreover, porous media are used to transport and store energy in many industrial applications, such as heat pipes, solid matrix heat exchangers, electronic cooling, and chemical reactors. An important characteristic for the combination of the fluid and the porous medium is the tortuosity, which represents the hindrance to flow diffusion imposed by local boundaries or local viscosity [12,13].

Motivated by these facts, the present work has been undertaken in order to analyze the fully developed flow of an incompressible, third-grade nanofluid in coaxial cylinders. Two illustrative models of variable viscosity, namely Reynolds' model and Vogel's model, are considered. Porous media are also taken into account. Since it is not easy to get an exact analytical solution of a nonlinear problem, we may go for analytic series solutions. To derive the solutions of nonlinear coupled equations, we have used one of the most modern methods, the homotopy analysis method (HAM) [14–18], which is particularly suitable for strongly nonlinear problems. Besides, unlike other analytic techniques [19–22], the HAM provides us with a simple way to ensure the convergence of series solutions of a nonlinear problem and does not require any small parameter. Convergence of the obtained series solutions are first properly discussed and then analytic solutions of the velocity profile, temperature profile, and mass concentration are developed by the HAM.

2. Formulation of the problem

Let us consider a steady, incompressible, third-grade nanofluid in coaxial cylinders. The stress in a third-grade fluid is given by

$$\mathbf{T} = -p\mathbf{I} + \mu\mathbf{A}_1 + \alpha_1\mathbf{A}_2 + \alpha_2\mathbf{A}_1^2 + \beta_1\mathbf{A}_3 + \beta_2(\mathbf{A}_1\mathbf{A}_2 + \mathbf{A}_2\mathbf{A}_1) + \beta_3(\operatorname{tr}\mathbf{A}_1^2)\mathbf{A}_1, \tag{1}$$

where μ is the coefficient of viscosity, and $\alpha_1, \alpha_2, \beta_1, \beta_2, \beta_3$ are the material moduli; all are functions of temperature in general. In the above representation, $-p\mathbf{I}$ is the spherical stress due to the constraint of incompressibility, and the kinematical tensors $\mathbf{A}_1$, $\mathbf{A}_2$ and $\mathbf{A}_3$ are defined by

$$\mathbf{A}_1 = (\operatorname{grad}\mathbf{V}) + (\operatorname{grad}\mathbf{V})^t, \tag{2}$$

$$\mathbf{A}_n = \frac{D\mathbf{A}_{n-1}}{Dt} + \mathbf{A}_{n-1}(\operatorname{grad}\mathbf{V}) + (\operatorname{grad}\mathbf{V})^t A_{n-1}, \quad n = 2, 3, \tag{3}$$

where $\mathbf{V} = [0, 0, v(r)]$ denotes the velocity field, grad is the gradient operator, and D/Dt is the material time derivative, which is defined by

$$\frac{D(\cdot)}{Dt} = \frac{\partial(\cdot)}{\partial t} + [\operatorname{grad}(\cdot)]\mathbf{V}, \tag{4}$$

where $\partial/\partial t$ is the partial derivative with respect to time. A detailed thermodynamic analysis of the model, represented by Eq. (1), is given in [23], where it is shown that, if all the motions of the fluid are to be compatible with thermodynamics in the sense that these motions satisfy the Clausius–Duhem inequality, and if it is assumed that the specific Helmholtz free energy is a minimum when the fluid is locally at rest, then

$$\mu \geq 0,\ \alpha_1 \geq 0, \quad |\alpha_1 + \alpha_2| \leq \sqrt{24\mu\beta_3}, \qquad \beta_1 = \beta_2 = 0, \qquad \beta_3 \geq 0. \tag{5}$$

In our analysis, we assume that the fluid is thermodynamically compatible, and therefore Eq. (1) reduces to

$$\mathbf{T} = -p_1\mathbf{I} + \mu\mathbf{A}_1 + \alpha_1\mathbf{A}_2 + \alpha_2\mathbf{A}_1^2 + \beta_3(\operatorname{tr}\mathbf{A}_1^2)\mathbf{A}_1. \tag{6}$$

It is noted that this constitutive relation not only predicts the normal stress differences, but also can predict the "shear-thickening" phenomenon (since $\beta_3 > 0$), which is the increase in viscosity with increasing shear rate. That is, we can rewrite Eq. (6) as

$$\mathbf{T} = -p_1\mathbf{I} + \left[\mu + \beta_3(\operatorname{tr}\mathbf{A}_1^2)\right]\mathbf{A}_1 + \alpha_1\mathbf{A}_2 + \alpha_2\mathbf{A}_1^2, \tag{7}$$

and then the quantity in the brackets can be thought of as an effective shear-dependent viscosity; that is, $\mu + \beta_3(\operatorname{tr}\mathbf{A}_1^2)$. Obviously a viscous fluid is governed by continuity and Navier–Stokes equations, which, when the fluid is incompressible,

take the form of the following four field equations, embodying the conservation of total mass, momentum, thermal energy, and nanoparticles, respectively,

$$\rho_f\left(\frac{\partial \mathbf{V}}{\partial t}+\mathbf{V}.\nabla\mathbf{V}\right)=\operatorname{div}\mathbf{T}-\frac{\mu\varphi}{k}\left(1+\lambda_r\frac{\partial}{\partial t}\right)\mathbf{V}+\left[\phi\rho_p+(1-\phi)\,\rho_f\left[1-\beta_T\left(\theta-\theta_w\right)\right]\right]\mathbf{g}, \tag{8}$$

$$(\rho c)_f\left(\frac{\partial\theta}{\partial t}+\mathbf{V}.\nabla\theta\right)=k\nabla^2\theta+(\rho c)_p\left[D_b\nabla\phi.\nabla\theta+\frac{D_T}{\theta_w}\nabla\theta.\nabla\theta\right], \tag{9}$$

$$\left(\frac{\partial\phi}{\partial t}+\mathbf{V}.\nabla\phi\right)=D_b\nabla^2\phi+\frac{D_T}{\theta_w}\nabla^2\theta, \tag{10}$$

along with the boundary conditions

$$v\left(R_1\right)=v_0,\qquad v\left(R_2\right)=0;\qquad \theta\left(R_1\right)=\theta_w,\qquad \theta\left(R_2\right)=0;\qquad \phi\left(R_1\right)=\phi_w,\qquad \phi\left(R_2\right)=0, \tag{11}$$

where θ is the temperature, ϕ is the nanoparticle volume fraction, ρ_f is the density of the base fluid, ρ_p is the density of the nanoparticles, $\mathbf{g}$ is the gravitational vector, β_T is the volumetric solutal expansion coefficient of the nanofluid, and R_1 and R_2 are the radii of the inner and outer cylinders respectively. The Brownian diffusion coefficient and the thermophoretic diffusion coefficient are respectively denoted by D_b and D_T. Moreover, λ_r, φ, and k are the retardation time, porosity, and permeability of the porous medium (for detailed analysis see [24]).

Let us introduce the following non-dimensional parameters:

$$\overline{v}=\frac{v}{V_0},\qquad \overline{r}=\frac{r}{R},\qquad \overline{\mu}=\frac{\mu}{\mu_0},\qquad \overline{\theta}=\frac{\theta-\theta_w}{\theta_m-\theta_w},\qquad \overline{\phi}=\frac{\phi-\phi_w}{\phi_m-\phi_w} \tag{12}$$

where v_0, μ_0, θ_w, θ_m, and ϕ_m denote the reference velocity, reference viscosity, pipe temperature, fluid temperature, and mass concentration, respectively. Substituting Eq. (6) in the balance of linear momentum and using the non-dimensional quantities given in Eq. (12), the dimensionless forms of the governing equations ((8) to (11)), after dropping bars for simplicity, lead to the following non-dimensional coupled equations:

$$\frac{d\mu}{dr}\frac{du}{dr}+\frac{\mu}{r}\frac{du}{dr}+\mu\frac{d^2u}{dr^2}+\frac{\Lambda}{r}\left(\frac{du}{dr}\right)^3+3\Lambda\left(\frac{du}{dr}\right)^2\frac{d^2u}{dr^2}=P\left[\mu+\Lambda\left(\frac{dv}{dr}\right)^2\right]v+c-G_r\theta-B_r\phi, \tag{13}$$

$$\alpha\left(\frac{d^2\theta}{dr^2}+\frac{1}{r}\frac{d\theta}{dr}\right)+N_b\frac{d\theta}{dr}\frac{d\phi}{dr}+\alpha_1N_t\left(\frac{d\theta}{dr}\right)^2=0, \tag{14}$$

$$N_b\left(\frac{d^2\theta}{dr^2}+\frac{1}{r}\frac{d\theta}{dr}\right)+N_t\left(\frac{d^2\phi}{dr^2}+\frac{1}{r}\frac{d\phi}{dr}\right)=0, \tag{15}$$

subject to boundary conditions

$$v(1)=1,\qquad v(2)=0;\qquad \theta(1)=1,\qquad \theta(2)=0;\qquad \phi(1)=1,\qquad \phi(2)=0. \tag{16}$$

The following dimensionless quantities are also obtained:

$$\left.\begin{aligned}&\Lambda=\frac{2\beta_3v_0^2}{\mu_0R^2},\qquad c=\frac{\frac{\partial\hat{p}}{\partial z}R^2}{v_0\mu_0},\qquad P=\frac{\varphi}{kR_2^2},\\&N_b=D_b\left(\phi_m-\phi_w\right),\qquad N_t=\frac{D_T\left(\theta_m-\theta_w\right)}{\theta_w},\\&G_r=\frac{\left(\theta_m-\theta_w\right)\rho_{fw}R^2\left(1-\phi_w\right)g}{\mu_0u_0},\qquad B_r=\frac{\left(\rho_p-\rho_w\right)R^2\left(\phi_m-\phi_w\right)g}{\mu_0u_0}\end{aligned}\right\}. \tag{17}$$

Here, Λ, P, c, G_r, B_r, N_t, and N_b are the third-grade parameter, porosity parameter, pressure gradient, thermophoresis diffusion constant, Brownian diffusion constant, thermophoresis parameter, and Brownian motion parameter, respectively.

3. Solution of the problem

In this section, the HAM solutions will be determined for the velocity, temperature, and nanoparticle concentration by using Reynolds' model and Vogel's model of viscosity.

Case I: *Reynolds' model*

Here, the viscosity is taken in the form

$$\mu=\mathbf{e}^{-B\,\theta}, \tag{18}$$

which, after using the Maclaurin's series, can be written as

$$\mu = 1 - \theta B + O(\theta^2). \tag{19}$$

For the HAM solution we select

$$v_0(r) = \frac{(128 - r^7)}{127}, \qquad \theta_0(r) = \frac{(128 - r^7)}{127}, \qquad \phi_0 = \frac{(128 - r^7)}{127} \tag{20}$$

as the initial approximation of v, , θ, and ϕ, respectively, which satisfy the following linear operator and corresponding boundary conditions:

$$\mathcal{L} = \frac{d^2}{dr^2}, \tag{21}$$

such that

$$\mathcal{L}[C_1 + C_2 \ln r] = 0, \tag{22}$$

where C_1 and C_2 are arbitrary constants.

From Eqs. (14) to (16), we also define the following nonlinear operators:

$$\left.\begin{aligned} \mathcal{N}_v[v^*(r,p), \theta^*(r,p), \phi^*(r,p)] = & -B\frac{d\theta^*}{dr}\frac{dv^*}{dr} + \frac{(1-\theta^*B)}{r}\frac{dv^*}{dr} + \frac{\Lambda}{r}\left(\frac{dv^*}{dr}\right)^3 \\ & + \left(1-\theta^*B\right)\frac{d^2v^*}{dr^2} + 3\Lambda\left(\frac{dv^*}{dr}\right)^2\frac{d^2v^*}{dr^2} + G_r\theta^* \\ & + B_r\phi^* - c - P\left[\left(1-\theta^*B\right) + \Lambda\left(\frac{dv^*}{dr}\right)^2\right]v^* \end{aligned}\right\}, \tag{23}$$

$$\mathcal{N}_\theta[v^*(r,p), \theta^*(r,p), \phi^*(r,p)] = \alpha\left(\frac{d^2\theta^*}{dr^2} + \frac{1}{r}\frac{d\theta^*}{dr}\right) + N_b\frac{d\theta^*}{dr}\frac{d\phi^*}{dr} + \alpha_1 N_t\left(\frac{d\theta^*}{dr}\right)^2, \tag{24}$$

$$\mathcal{N}_\phi[v^*(r,p), \theta^*(r,p), \phi^*(r,p)] = N_b\left(\frac{d^2\theta^*}{dr^2} + \frac{1}{r}\frac{d\theta^*}{dr}\right) + N_t\left(\frac{d^2\phi^*}{dr^2} + \frac{1}{r}\frac{d\phi^*}{dr}\right), \tag{25}$$

and then construct the homotopy

$$\mathcal{H}_v[v^*(r,p)] = (1-p)\mathcal{L}[v^*(r,p) - v_0(r)] - p\hbar\mathcal{N}_v[v^*(r,p), \theta^*(r,p), \phi^*(r,p)], \tag{26}$$

$$\mathcal{H}_\theta[\theta^*(r,p)] = (1-p)\mathcal{L}[\theta^*(r,p) - v_0(r)] - p\hbar\mathcal{N}_\theta[v^*(r,p), \theta^*(r,p), \phi^*(r,p)], \tag{27}$$

$$\mathcal{H}_\phi[v^*(r,p)] = (1-p)\mathcal{L}[\phi^*(r,p) - v_0(r)] - p\hbar\mathcal{N}_\phi[v^*(r,p), \theta^*(r,p), \phi^*(r,p)], \tag{28}$$

where the embedding parameter $p \in [0, 1]$, and $\hbar$ is a non-zero auxiliary parameter. Setting $\mathcal{H}_v[v^*(r,p)] = \mathcal{H}_\theta[\theta^*(r,p)] = \mathcal{H}_\phi[\phi^*(r,p)] = 0$, the zeroth-order deformation equations are given by the following relations:

$$(1-p)\mathcal{L}[v^*(r,p) - v_0(r)] = p\hbar\mathcal{N}_v[v^*(r,p), \theta^*(r,p), \phi^*(r,p)], \tag{29}$$

$$(1-p)\mathcal{L}[\theta^*(r,p) - \theta_0(r)] = p\hbar\mathcal{N}_\theta[\theta^*(r,p), \theta^*(r,p), \phi^*(r,p)], \tag{30}$$

$$(1-p)\mathcal{L}[\phi^*(r,p) - \phi_0(r)] = p\hbar\mathcal{N}_\phi[\phi^*(r,p), \theta^*(r,p), \phi^*(r,p)], \tag{31}$$

$$v^*(1,p) = 1, \qquad \theta^*(1,p) = 1, \qquad \phi^*(1,p) = 1, \qquad v^*(2,p) = 0, \qquad \theta^*(2,p) = 0, \qquad \phi^*(2,p) = 0. \tag{32}$$

The mth-order deformation problems of above equations are

$$\mathcal{L}\left[v_m - \chi_m v_{m-1}\right] = \hbar\mathcal{R}1_m(r), \tag{33}$$

$$\mathcal{L}\left[\theta_m - \chi_m\theta_{m-1}\right] = \hbar\mathcal{R}2_m(r) \tag{34}$$

$$\mathcal{L}\left[\phi_m - \chi_m\phi_{m-1}\right] = \hbar\mathcal{R}3_m(r), \tag{35}$$

$$v_m(1) = 1, \qquad v_m(2) = 0, \qquad \theta_m(1) = 1, \qquad \theta_m(2) = 0, \qquad \phi_m(1) = 1, \qquad \phi_m(2) = 0, \tag{36}$$

where

$$\left.\begin{aligned} \mathcal{R}1_m(r) = & \frac{d^2v_{m-1}}{dr^2} + \frac{1}{r}\frac{dv_{m-1}}{dr} - B\sum_{k=0}^{m-1}\frac{dv_{m-1-k}}{dr}\frac{d\theta_k}{dr} - B\sum_{k=0}^{m-1}\frac{dv_{m-1-k}}{dr}\theta_k - B\sum_{k=0}^{m-1}\frac{d^2v_{m-1-k}}{dr^2}\theta_k \\ & + \frac{\Lambda}{r}\sum_{k=0}^{m-1}\sum_{l=0}^{k}\left(\frac{dv_{m-1-k}}{dr}\right)\frac{dv_{m-k-l}}{dr}\frac{dv_l}{dr} + 3\Lambda\sum_{k=0}^{m-1}\sum_{l=0}^{k}\left(\frac{dv_{m-1-k}}{dr}\right)\frac{dv_{m-k-l}}{dr}\frac{d^2v_l}{dr^2} \\ & - Pv_{m-1} + BP\sum_{k=0}^{m-1}v_{m-1-k}\theta_k - P\Lambda\sum_{k=0}^{m-1}\sum_{l=0}^{k}\left(\frac{dv_{m-1-k}}{dr}\right)\frac{dv_{m-k-l}}{dr}v_l \\ & - c(1-\chi_m) + G_r\theta_{m-1} + B_r\phi_{m-1} \end{aligned}\right\}, \tag{37}$$

$$\mathcal{R}2_m(r) = \alpha\left(\frac{d^2\theta_{m-1}}{dr^2} + \frac{1}{r}\frac{d\theta_{m-1}}{dr}\right) + N_b\sum_{k=0}^{m-1}\frac{d\theta_{m-1-i}}{dr}\frac{d\phi_i}{dr} + \alpha_1 N_t\sum_{k=0}^{m-1}\frac{d\theta_{m-1-i}}{dr}\frac{d\theta_i}{dr}, \tag{38}$$

$$\mathcal{R}3_m(r) = N_b\left(\frac{d^2\theta_{m-1}}{dr^2} + \frac{1}{r}\frac{d\theta_{m-1}}{dr}\right) + N_t\left(\frac{d^2\phi_{m-1}}{dr^2} + \frac{1}{r}\frac{d\phi_{m-1}}{dr}\right) \tag{39}$$

are recurrence formulae, in which

$$\chi_m = \begin{cases} 0, & m \le 1, \\ 1, & m > 1. \end{cases} \tag{40}$$

Case II: *Vogel's model*

$$\mu = \mu_0 \mathbf{e}^{\left(\frac{A}{B+\theta} - \theta_0\right)}, \tag{41}$$

or Eq. (41) can be approximated [25] as

$$\mu = \frac{c}{S}\left(1 - \frac{\theta A}{B^2}\right) \quad \text{where } S = \mu_o e^{\left(\frac{A}{B} - \theta_0\right)}. \tag{42}$$

For HAM solution here we select the initial guess and linear operator given in Eqs. (20) and (21), respectively. With the same procedure as given in case I, the zeroth-order and mth-order deformation equations are respectively given by the following relations:

$$(1-p)\mathcal{L}[v^*(r,p) - v_0(r)] = p\hbar\mathcal{N}_v[v^*(r,p), \theta^*(r,p), \phi^*(r,p)], \tag{43}$$

$$(1-p)\mathcal{L}[\theta^*(r,p) - \theta_0(r)] = p\hbar\mathcal{N}_\theta[\theta^*(r,p), \theta^*(r,p), \phi^*(r,p)], \tag{44}$$

$$(1-p)\mathcal{L}[\phi^*(r,p) - \phi_0(r)] = p\hbar\mathcal{N}_\phi[\phi^*(r,p), \theta^*(r,p), \phi^*(r,p)], \tag{45}$$

$$v^*(1,p) = 1, \quad \theta^*(1,p) = 1, \quad \phi^*(1,p) = 1, \quad v^*(2,p) = 0, \quad \theta^*(2,p) = 0, \quad \phi^*(2,p) = 0 \tag{46}$$

and

$$\mathcal{L}[v_m - \chi_m v_{m-1}] = \hbar\mathcal{R}4_m(r), \tag{47}$$

$$\mathcal{L}[\theta_m - \chi_m\theta_{m-1}] = \hbar\mathcal{R}5_m(r), \tag{48}$$

$$\mathcal{L}[\phi_m - \chi_m\phi_{m-1}] = \hbar\mathcal{R}6_m(r), \tag{49}$$

$$v_m(1) = 1, \quad v_m(2) = 0, \quad \theta_m(1) = 1, \quad \theta_m(2) = 0, \quad \phi_m(1) = 1, \quad \phi_m(2) = 0, \tag{50}$$

where

$$\mathcal{N}_v[v^*(r,p), \theta^*(r,p), \phi^*(r,p)] = \left.\begin{aligned} &-\frac{cA}{SB^2}\frac{d\theta^*}{dr}\frac{dv^*}{dr} + \frac{c}{rS}\left(1 - \frac{\theta^* A}{B^2}\right)\frac{dv^*}{dr} \\ &+ \frac{c}{S}\left(1 - \frac{\theta^* A}{B^2}\right)\frac{d^2v^*}{dr^2} + \frac{\Lambda}{r}\left(\frac{dv^*}{dr}\right)^3 \\ &+ 3\Lambda\left(\frac{dv^*}{dr}\right)^2\frac{d^2v^*}{dr^2} - c + G_r\theta^* \\ &+ B_r\phi^* - P\left[\left(1 - \frac{\theta^* A}{B^2}\right) + \Lambda\left(\frac{dv^*}{dr}\right)^2\right]v^* \end{aligned}\right\}, \tag{51}$$

$$\mathcal{N}_\theta[v^*(r,p), \theta^*(r,p), \phi^*(r,p)] = \alpha\left(\frac{d^2\theta^*}{dr^2} + \frac{1}{r}\frac{d\theta^*}{dr}\right) + N_b\frac{d\theta^*}{dr}\frac{d\phi^*}{dr} + \alpha_1 N_t\left(\frac{d\theta^*}{dr}\right)^2, \tag{52}$$

$$\mathcal{N}_\phi[v^*(r,p), \theta^*(r,p), \phi^*(r,p)] = N_b\left(\frac{d^2\theta^*}{dr^2} + \frac{1}{r}\frac{d\theta^*}{dr}\right) + N_t\left(\frac{d^2\phi^*}{dr^2} + \frac{1}{r}\frac{d\phi^*}{dr}\right), \tag{53}$$

$$\left.\begin{aligned}\mathcal{R}4_m(r) = {} & \frac{c}{S}\frac{d^2v_{m-1}}{dr^2} + \frac{c}{rS}\frac{dv_{m-1}}{dr} - \frac{cA}{SB^2}\sum_{k=0}^{m-1}\frac{dv_{m-1-k}}{dr}\frac{d\theta_k}{dr} \\ & - \frac{cA}{rSB^2}\sum_{k=0}^{m-1}\frac{dv_{m-1-k}}{dr}\theta_k - \frac{cA}{B^2}\sum_{k=0}^{m-1}\frac{d^2v_{m-1-k}}{dr^2}\theta_k \\ & + \frac{\Lambda}{r}\sum_{k=0}^{m-1}\sum_{l=0}^{k}\left(\frac{dv_{m-1-k}}{dr}\right)\frac{dv_{m-k-l}}{dr}\frac{dv_l}{dr} - P\frac{c}{S}v_{m-1} \\ & + 3\Lambda\sum_{k=0}^{m-1}\sum_{l=0}^{k}\left(\frac{dv_{m-1-k}}{dr}\right)\frac{dv_{m-k-l}}{dr}\frac{d^2v_l}{dr^2} + \frac{PAc}{B^2S}\sum_{k=0}^{m-1}v_{m-1-k}\theta_k + G_r\theta_{m-1} + B_r\phi_{m-1} \\ & - P\Lambda\sum_{k=0}^{m-1}\sum_{l=0}^{k}\left(\frac{dv_{m-1-k}}{dr}\right)\frac{dv_{m-k-l}}{dr}v_l - c(1-\chi_m)\end{aligned}\right\}, \tag{54}$$

$$\mathcal{R}5_m(r) = \alpha\left(\frac{d^2\theta_{m-1}}{dr^2} + \frac{1}{r}\frac{d\theta_{m-1}}{dr}\right) + N_b\sum_{k=0}^{m-1}\frac{d\theta_{m-1-i}}{dr}\frac{d\phi_i}{dr} + \alpha_1N_t\sum_{k=0}^{m-1}\frac{d\theta_{m-1-i}}{dr}\frac{d\theta_i}{dr}, \tag{55}$$

$$\mathcal{R}6_m(r) = N_b\left(\frac{d^2\theta_{m-1}}{dr^2} + \frac{1}{r}\frac{d\theta_{m-1}}{dr}\right) + N_t\left(\frac{d^2\phi_{m-1}}{dr^2} + \frac{1}{r}\frac{d\phi_{m-1}}{dr}\right). \tag{56}$$

In both cases, for $p = 0$ and $p = 1$, we have

$$\left.\begin{aligned} v^*(r;0) &= v_0(r), \quad \theta^*(r;0) = \theta_0(y), \quad \phi^*(r;0) = \phi_0(r) \\ v^*(r;1) &= v(r), \quad \theta^*(r;1) = \theta(r) \quad \phi^*(r;1) = \phi(r)\end{aligned}\right\}. \tag{57}$$

When p increases from 0 to 1 then in view of Eq. (57), the mth-order solutions in terms of Taylor's series can be written as

$$\left.\begin{aligned} v^*(r,p) &= v_0(r) + \sum_{m=1}^{\infty}v_m(r)p^m \\ \theta^*(r,p) &= \theta_0(r) + \sum_{m=1}^{\infty}\theta_m(r)p^m \\ \phi^*(r,p) &= \phi_0(r) + \sum_{m=1}^{\infty}\phi_m(r)p^m\end{aligned}\right\}, \tag{58}$$

where

$$v_m(r) = \frac{1}{m!}\frac{\partial^m v^*(r,p)}{\partial p^m}\bigg|_{p=0}, \qquad \theta_m(r) = \frac{1}{m!}\frac{\partial^m\theta^*(r,p)}{\partial p^m}\bigg|_{p=0} \qquad \phi_m(r) = \frac{1}{m!}\frac{\partial^m\phi^*(r,p)}{\partial p^m}\bigg|_{p=0}. \tag{59}$$

The convergence of Eq. (58) depends upon $\hbar$; therefore, we choose $\hbar$ in such a way that it should be convergent at $p = 1$. In view of Eq. (57), finally we have

$$v(r) = v_0(r) + \sum_{m=1}^{\infty}v_m(r), \qquad \theta(r) = \theta_0(r) + \sum_{m=1}^{\infty}\theta_m(r), \qquad \phi(r) = \phi_0(r) + \sum_{m=1}^{\infty}\phi_m(r). \tag{60}$$

4. Convergence of the solution

It is noticed that the explicit, analytical expressions (29)–(36), and (43)–(50) contain the auxiliary parameter $\hbar$. As pointed out by Liao [26], the convergence region and rate of approximations given by the HAM are strongly dependent upon $\hbar$. Figs. 1–3 portray the $\hbar$-curves to find the range of $\hbar$ for Reynolds' model for velocity, temperature, and nanoparticle concentration, respectively. The range for admissible values of $\hbar$ for velocity is $-0.3 \le \hbar \le -0.1$, for temperature is $-1.9 \le \hbar \le -0.1$ and for nanoparticle concentration profile is $-2 \le \hbar \le -0.5$. Figs. 4–6 represent the $\hbar$-curves for Vogel's model. The admissible ranges for the velocity profile, temperature profile, and nanoparticle concentration are $-0.1 \le \hbar \le -0.01$, $-1.9 \le \hbar \le -0.5$, and $-1.9 \le \hbar \le -0.1$, respectively.

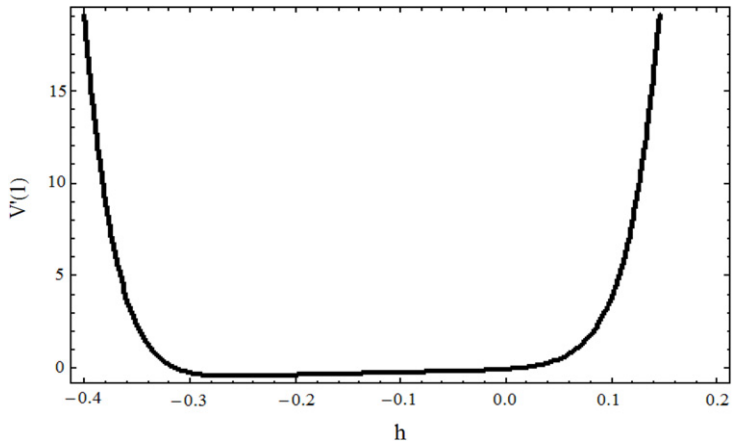

Fig. 1. $\hbar$-curve for the velocity profile for Reynolds' model at 15th order approximation.

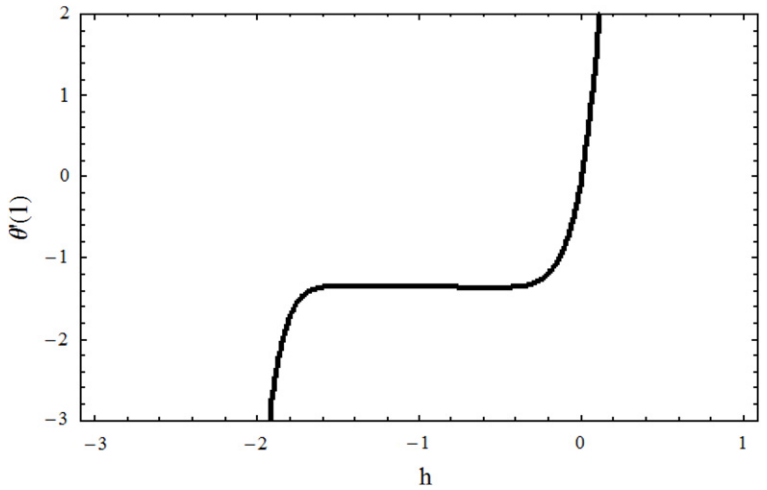

Fig. 2. $\hbar$-curve for the temperature profile for Reynolds' model at 15th order approximation.

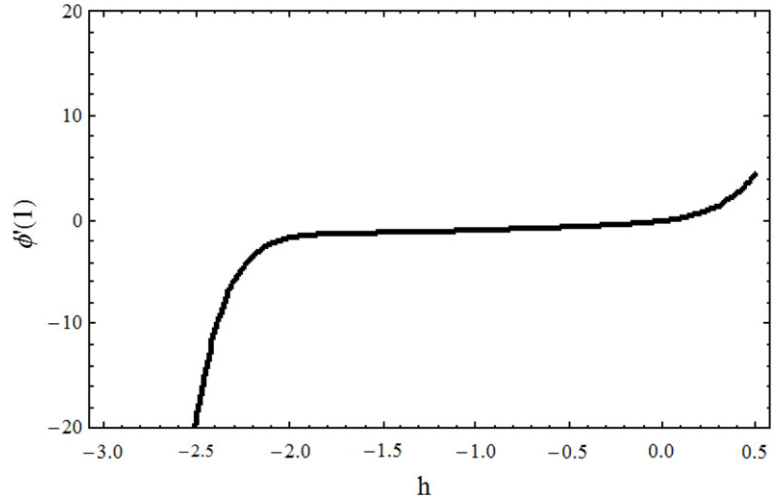

Fig. 3. $\hbar$-curve for the nanoparticle concentration profile for Reynolds' model at 15th order approximation.

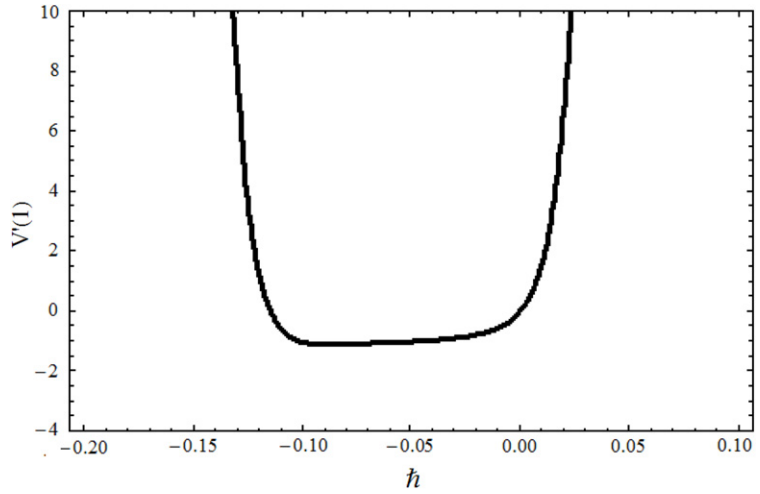

Fig. 4. $\hbar$-curve for the velocity profile for Vogel's model at 15th order approximation.

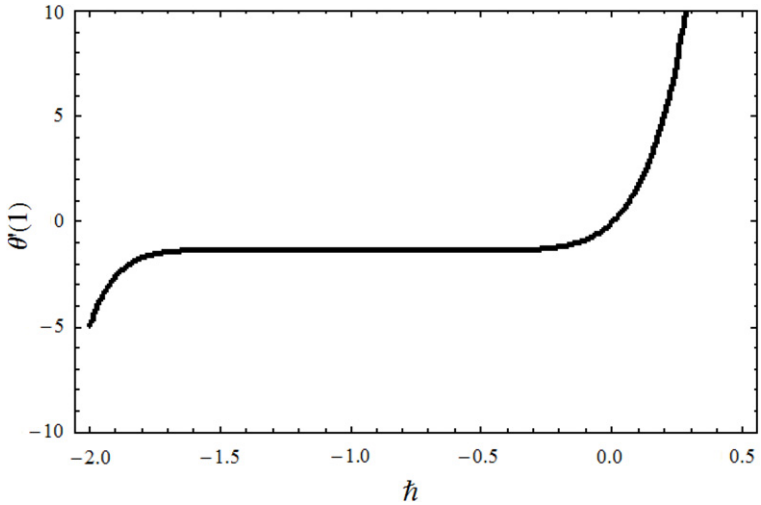

Fig. 5. $\hbar$-curve for the temperature profile for Vogel's model at 15th order approximation.

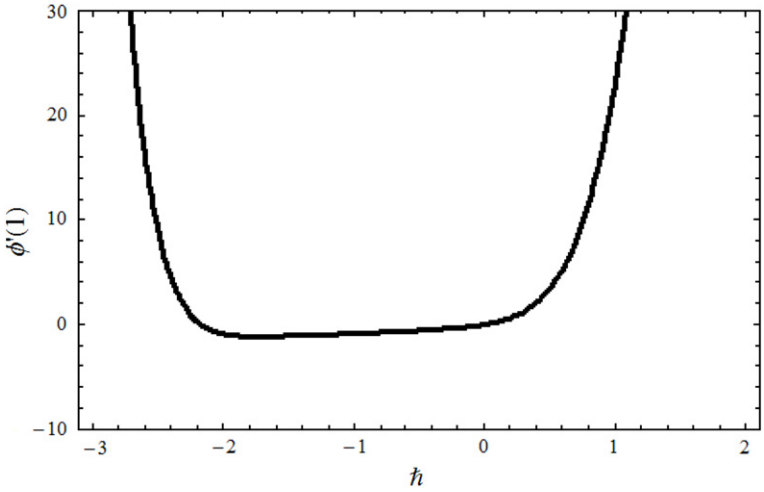

Fig. 6. $\hbar$-curve for the nanoparticle concentration profile for Vogel's model at 15th order approximation.

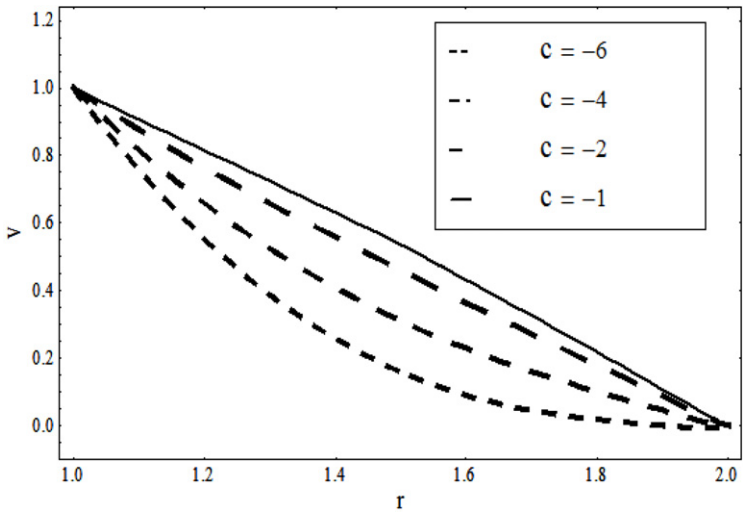

Fig. 7. Influence of c on velocity for Reynolds' model when $\Lambda = 0.1$ and $P = N_t = N_b = 1$.

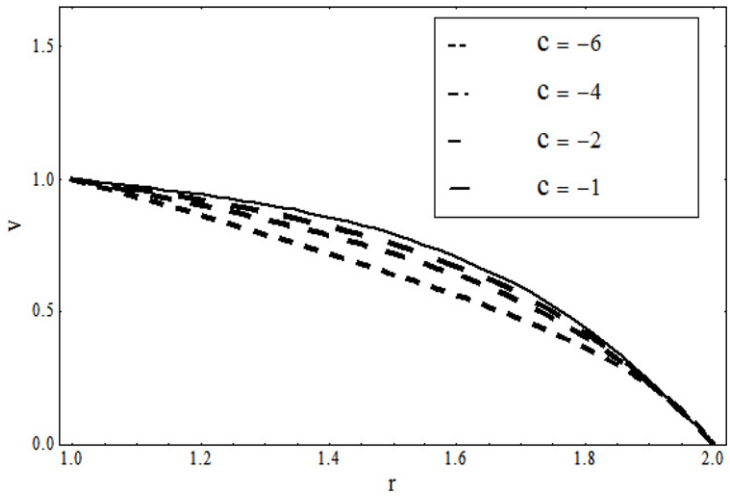

Fig. 8. Influence of c on velocity for Vogel's model when $\Lambda = 0.1$ and $P = N_t = N_b = 1$.

5. Results and discussion

To see the effects of the emerging parameters for Reynolds' model and Vogel's model on the velocity, temperature, and nanoparticle concentration Figs. 7–22 have been provided. The effects of pressure gradient c, third-grade parameter Λ, and porosity parameter P on the velocity are shown in Figs. 7–12. Figs. 13–22 show the effects of the thermophoresis parameter N_t and Brownian diffusion coefficient N_b on the velocity, temperature, and nanoparticle concentration profiles.

In Figs. 7 and 12, it is found that the velocity decreases by an increase in pressure gradient c, third-grade parameter Λ, and porosity parameter P. Figs. 13–24 show the influence of the thermophoresis parameter and Brownian diffusion coefficient on the velocity, temperature, and nanoparticle concentration. These figures show that the velocity, temperature, and nanoparticle concentration decrease by increasing the thermophoresis parameter when the Brownian diffusion coefficient is fixed and behave in an opposite manner when one varies the Brownian diffusion coefficient keeping the thermophoresis parameter fixed. This is accordance with the fact that for a thermal boundary the effects of the thermophoresis parameter and the Brownian diffusion coefficient are different.

6. Concluding remarks

In this paper, we have considered Reynolds' model and Vogel's model of viscosity for a third-grade nanofluid in a coaxial cylinder. The governing equations are coupled and nonlinear. The solutions for both models have been calculated using the homotopy analysis method. These solutions are valid not only for small but also for large values of all emerging parameters.

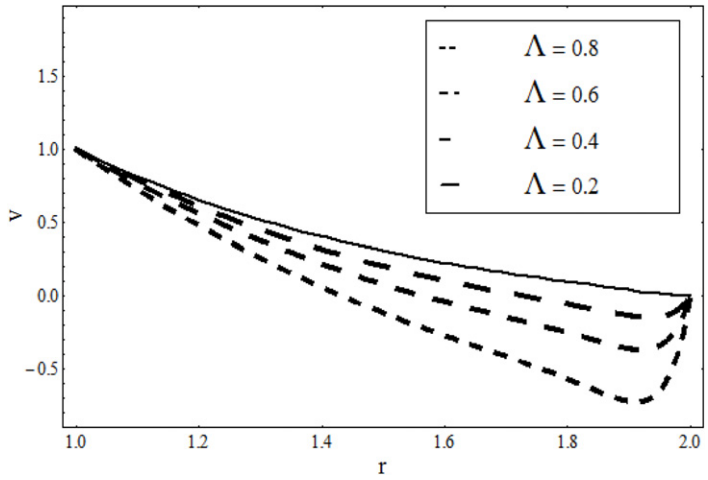

Fig. 9. Influence of Λ on velocity for Reynolds' model when $c = -4$ and $P = N_t = N_b = 1$.

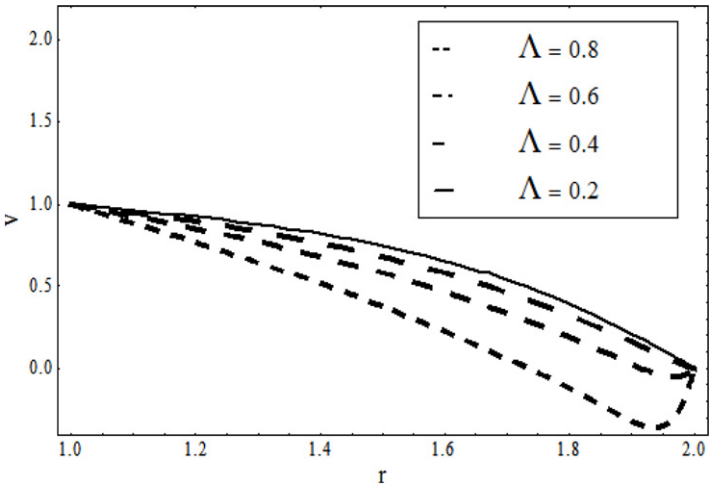

Fig. 10. Influence of Λ on velocity for Vogel's model when $c = -4$ and $P = N_t = N_b = 1$.

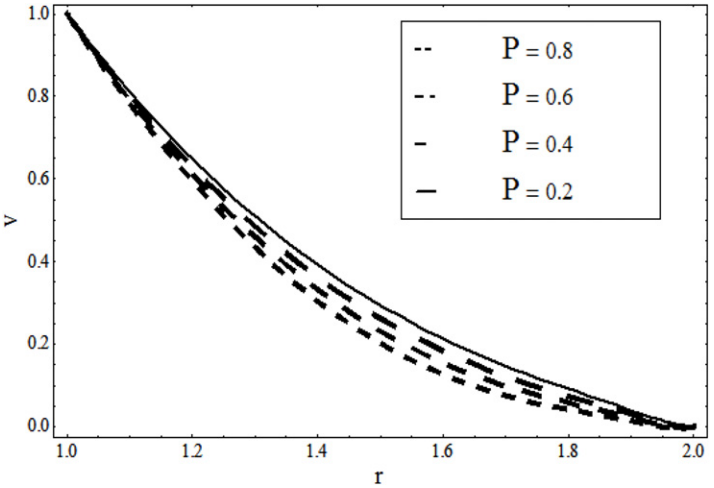

Fig. 11. Influence of P on velocity for Reynolds' model when $c = -4$, $\Lambda = 0.1$, and $P = N_t = N_b = 1$.

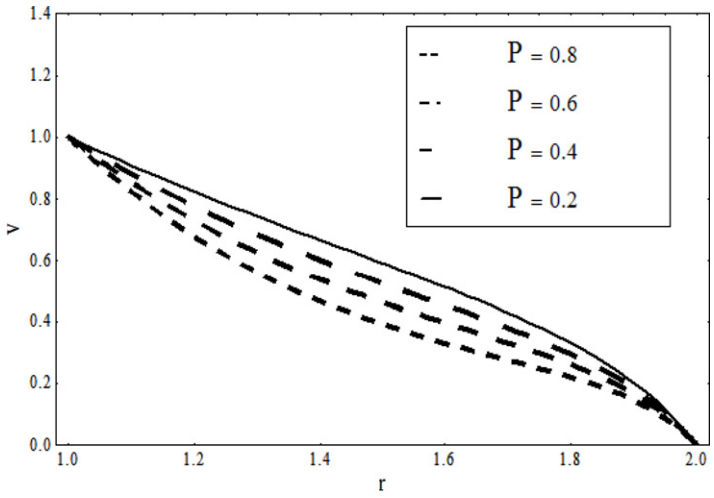

Fig. 12. Influence of P on velocity for Vogel's model when $c = -4$, $\Lambda = 0.1$, and $P = N_t = N_b = 1$.

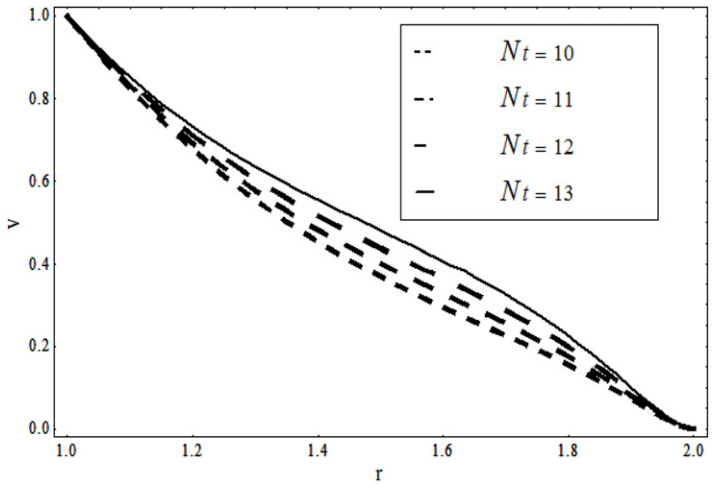

Fig. 13. Influence of N_t on velocity for Reynolds' model when $c = -4$, $\Lambda = 0.1$, and $N_b = P = 1$.

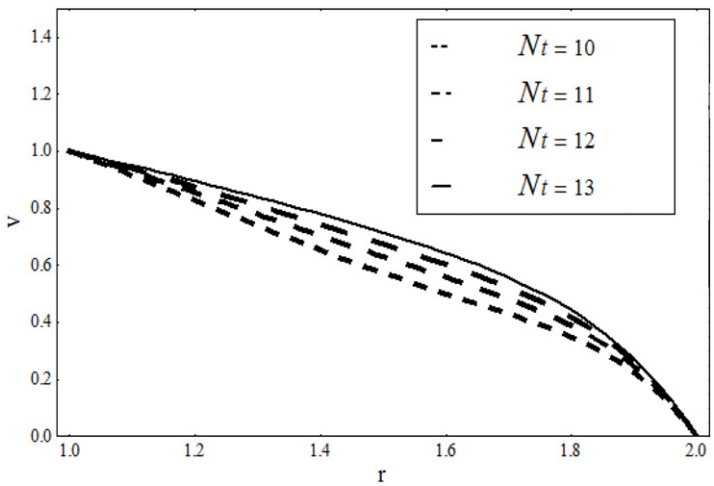

Fig. 14. Influence of N_t on velocity for Vogel's model when $c = -4$, $\Lambda = 0.1$, and $N_b = P = 1$.

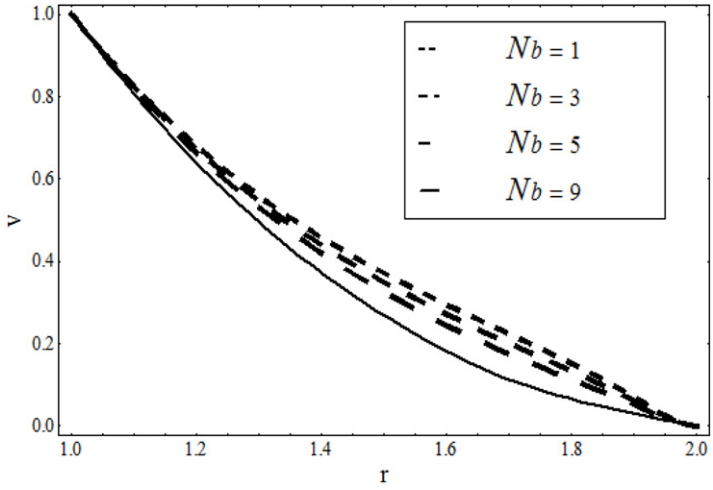

Fig. 15. Influence of N_b on velocity for Reynolds' model when $c = -4$, $\Lambda = 0.1$, and $N_t = P = 1$.

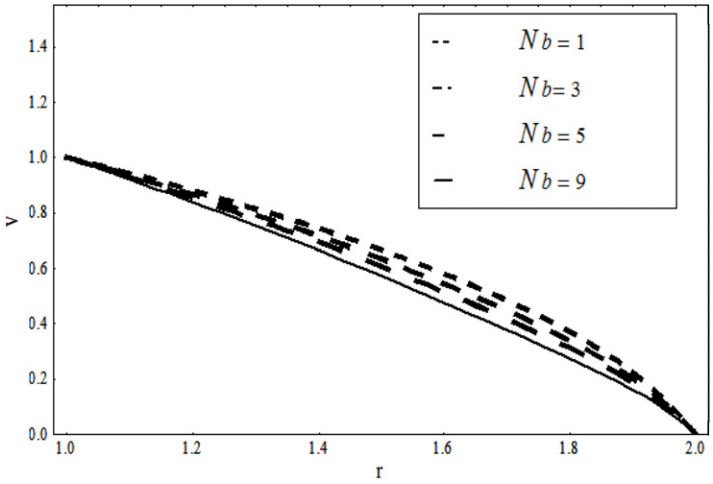

Fig. 16. Influence of N_t on velocity for Vogel's model when $c = -4$, $\Lambda = 0.1$, and $N_b = P = 1$.

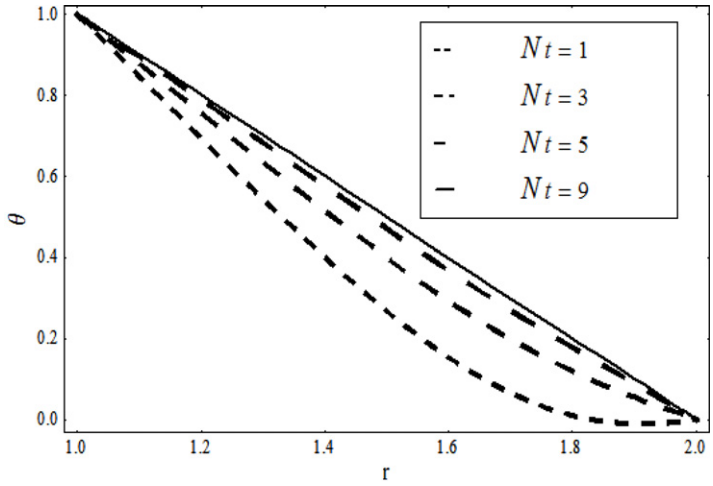

Fig. 17. Influence of N_t on temperature for Reynolds' model when $N_b = 1$.

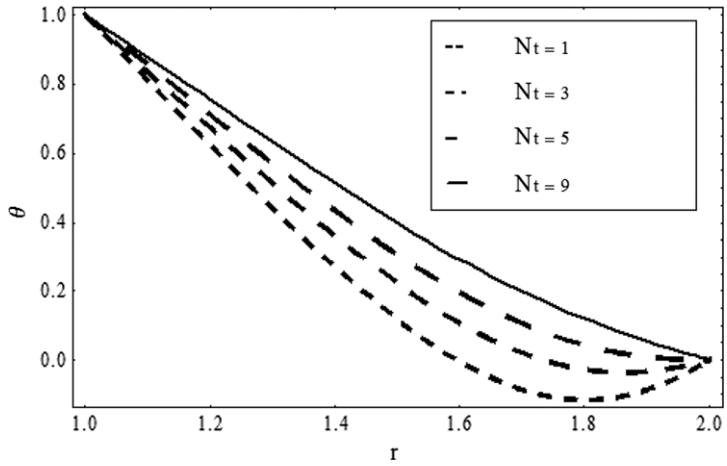

Fig. 18. Influence of N_t on temperature for Vogel's model when $N_b = 1$.

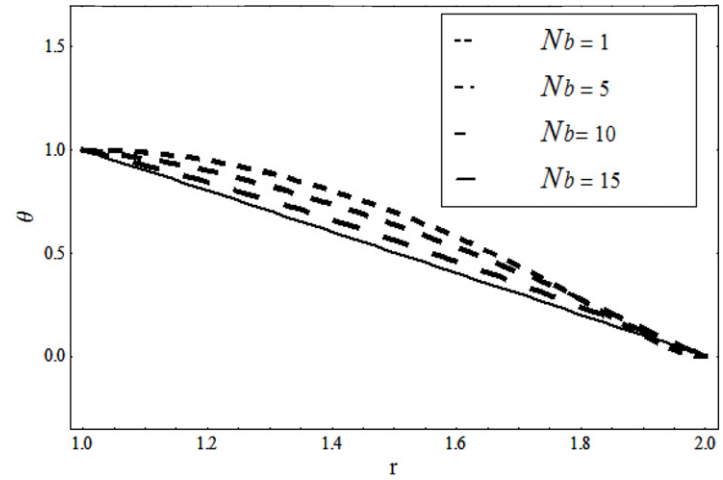

Fig. 19. Influence of N_b on temperature for Reynolds' model when $N_t = 1$.

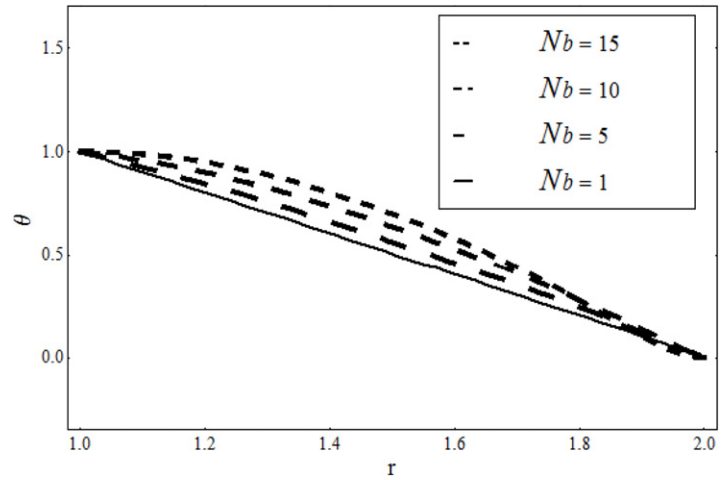

Fig. 20. Influence of N_t on temperature for Vogel's model when $N_t = 1$.

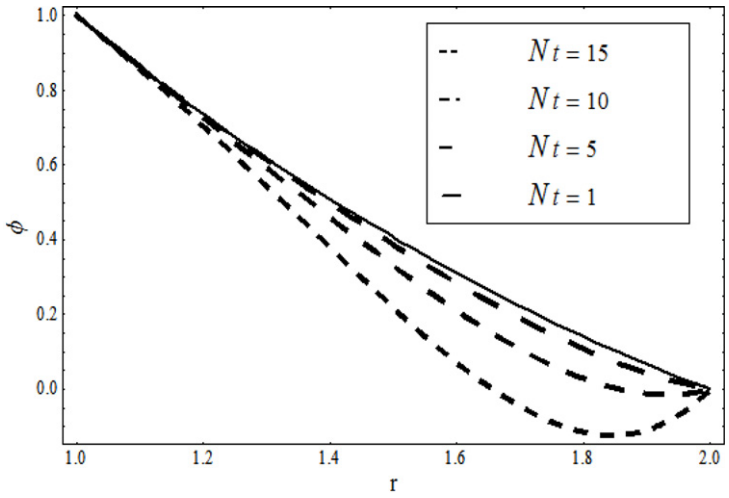

Fig. 21. Influence of N_t on nanoparticle concentration for Reynolds' model when $N_b = 1$.

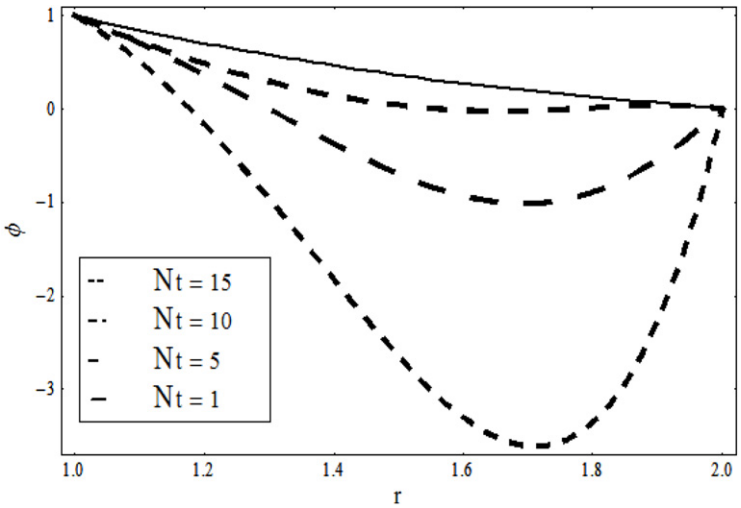

Fig. 22. Influence of N_t on nanoparticle concentration for Vogel's model when $N_b = 1$.

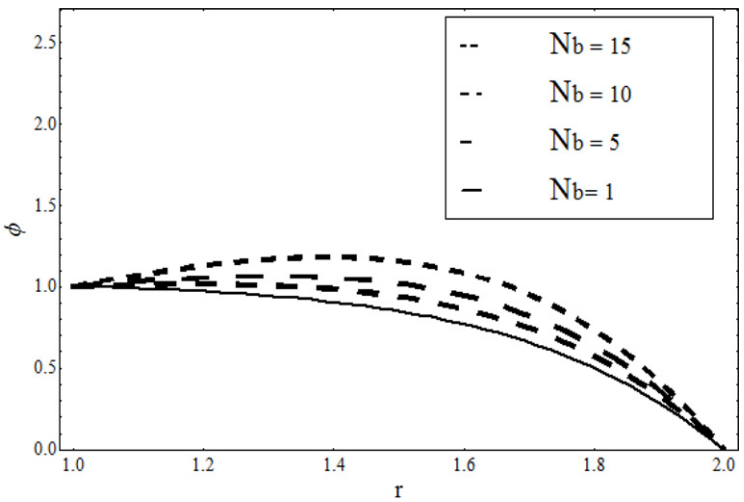

Fig. 23. Influence of N_b on nanoparticle concentration for Reynolds' model when $N_t = 1$.

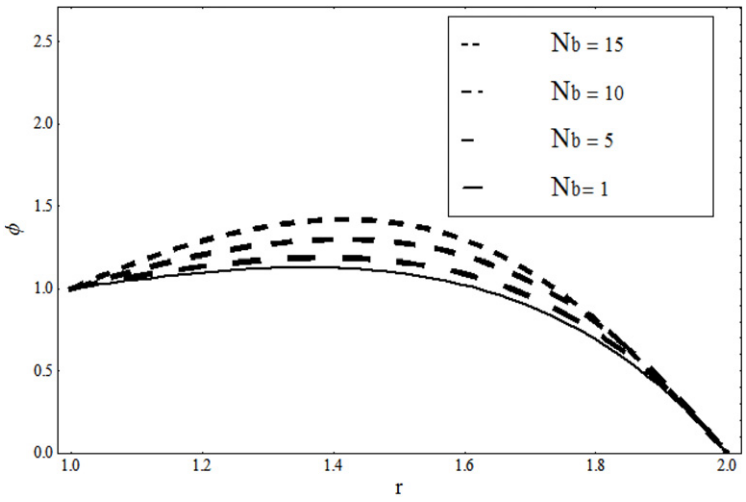

Fig. 24. Influence of N_b on nanoparticle concentration for Vogel's model when $N_t = 1$.

Porosity is also taken into account. The solutions valid for non-Newtonian parameters can be derived as special cases of the present analysis; for instance, when $G_r = B_r = 0$, then one recovers the case presented in [27] for the constant viscosity model. The analytical results of [28] for Reynolds' model and Vogel's model can be obtained by taking $P = G_r = B_r = 0$. It may be remarked that the problem for this particular model was not solved earlier even by any traditional perturbation technique. To the best of our knowledge, no such analysis is available in the literature which can simultaneously describe the heat transfer and porosity effects on variable viscosity for a non-Newtonian nanofluid. The results presented in this paper will now be available for experimental verification to give confidence for the well-posedness of this nonlinear boundary value problem.

Acknowledgments

R. Ellahi thanks the United State Education Foundation Pakistan and CIES USA, which honored him with a Fulbright Scholar Award for the year 2011–2012. He is also grateful to the Higher Education Commission and PCST of Pakistan for granting him NRPU and Productive Scientist awards, respectively.

References

[1] W.C. Tan, T. Masuoka, Stokes' first problem for a second grade fluid in a porous half space with heated boundary, Internat. J. Non-Linear Mech. 40 (2005) 512–522.
[2] W.C. Tan, T. Masuoka, Stability analysis of a Maxwell fluid in a porous medium heated from below, Phys. Lett. A 360 (2007) 454–460.
[3] F.M. Mahomed, T. Hayat, Note on an exact solution for the pipe flow of a third grade fluid, Acta Mech. 190 (2007) 233–236.
[4] M. Hameed, S. Nadeem, Unsteady MHD flow of a non-Newtonian fluid on a porous plate, J. Math. Anal. Appl. 325 (2007) 724–733.
[5] M.Y. Malik, A. Hussain, S. Nadeem, Flow of a Jeffrey—six constant fluid between coaxial cylinders with heat transfer, Commun. Theor. Phys. 56 (2011) 345–351.
[6] M.Y. Malik, A. Hussain, S. Nadeem, Analytical treatment of an Oldroy 8 constant fluid between the coaxial cylinder with variable viscosity, Commun. Theor. Phys. 56 (2011) 933–938.
[7] M.Y. Malik, A. Hussain, S. Nadeem, T. Hayat, Flow of a third grade fluid between coaxial cylinders with variable viscosity, Z. Naturforsch. A 64 (2009) 588–596.
[8] S.U.S. Choi, Nanofluids: from vision to reality through research, J. Heat Transfer 131 (2009) 1–9.
[9] S.U.S. Choi, J.A. Eastman, Enhancing thermal conductivity of fluids with nanoparticles, in: The proceedings of the ASME International Mechanical Engineering Congress and Exposition, ASME, San Francisco, vol. 66, 1995, pp. 99–105.
[10] K. Khanafer, K. Vafai, A critical synthesis of thermophysical characteristics of nanofluids, Int. J. Heat Mass Transfer 54 (2011) 4410–4428.
[11] K.V. Wong, O. Leon, Applications of nanofluids: current and future, Adv. Mech. Eng. 2010 (2010) 1–11.
[12] K. Vafai, Porous Media: Applications in Biological Systems and Biotechnology, Taylor & Francis, 2011.
[13] K. Vafai, S.J. Kim, Forced convection in a channel filled with porous medium—an exact solution, ASME J. Heat Transfer 111 (1989) 1103–1106.
[14] S.J. Liao, The proposed homotopy analysis technique for the solution of nonlinear problems, Ph.D. Thesis, Shanghai Jiao Tong University, 1992.
[15] S.J. Liao, On the homotopy analysis method for nonlinear problems, Appl. Math. Comput. 147 (2004) 499–513.
[16] S.J. Liao, A. Campo, Analytic solutions of the temperature distribution in Blasius viscous flow problems, J. Fluid Mech. 453 (2002) 411–425.
[17] T. Hayat, R. Ellahi, P.D. Ariel, S. Asghar, Homotopy solution for the channel flow of a third grade fluid, Nonlinear Dynam. 45 (2006) 55–64.
[18] R. Ellahi, Effect of the slip boundary condition on non-Newtonian flows in a channel, Commun. Nonlinear Sci. Numer. Simul. 14 (2009) 1377–1384.
[19] A.H. Nayfeh, Introduction to Perturbation Techniques, Wiley, New York, 1979.
[20] G.A. Adomian, Review of the decomposition method in applied mathematics, J. Math. Anal. Appl. 135 (1998) 501–544.
[21] V. Marinca, Application of modified homotopy perturbation method to nonlinear oscillations, Arch. Mech. 58 (2006) 241–256.
[22] M. Dehghan, F. Shakeri, The numerical solution of second Painlevé equation, Numer. Methods Partial Differential Equations 25 (2009) 1238–1259.
[23] R.L. Fosdick, K.R. Rajagopal, Thermodynamics and stability of fluids of third grade, Proc. R. Soc. Lond. Ser. A 339 (1980) 351–377.
[24] W.C. Tan, T. Masuoka, Stokes first problem for an Oldroyd-B fluid in a porous half space, Phys. Fluids 17 (2005) 023101–023107.

[25] M. Pakdemirli, B.S. Yilbas, Entropy generation for pipe flow of a third grade fluid with Vogel model viscosity, Internat. J. Non-Linear Mech. 41 (2006) 432–437.
[26] S.J. Liao, Beyond Perturbation: Introduction to Homotopy Analysis Method, Chapman & Hall, Boca Raton, 2003.
[27] R. Ellahi, S. Afzal, Effects of viscosity in a third grade fluid with porous medium: an analytic solution, Commun. Nonlinear Sci. Numer. Simul. 14 (2009) 2056–2072.
[28] M. Massoudi, I. Christie, Effects of variable viscosity and viscous dissipation on the flow of a third grade fluid in a pipe, Internat. J. Non-Linear Mech. 30 (1995) 687–699.